Chalcogenide Letters Vol. 13, No. 2, February 2016, p. 46 - 53

STUDIES ON STRUCTURAL, OPTICAL AND ELECTRICAL PROPERTIES OF $CuSbS_2$ NANOPARTICLES

B. SHU, Q. HAN*
Key Laboratory of Optoelectronics Materials and Devices, Shanghai Normal University, Shanghai, China

Recently, chalcostibite $CuSbS_2$ has been proposed as an alternative earth-abundant absorber material for thin film solar cells. $CuSbS_2$ nanoparticles successfully synthesized via hot-injection method using oleylamine (OLA) as solvents were reported in this paper. The $CuSbS_2$ nanoparticles with the average diameter about 15 nm possess a band gap of 1.26 eV. The photocurrent of film treated with anhydrous ethylenediamine solution (253 μA at 0.5 V bias) is much larger than the sample annealed at 300 ºC (13 μA at 0.5 V bias) indicates a higher conductivity of the film treated with anhydrous ethylenediamine solution compared to the thermal annealing sample. The higher photocurrent and proper band gap demonstrate that $CuSbS_2$ nanoparticles are indeed a very promising material for solar cell application.

(Received December 18, 2015; Accepted February 2, 2016)

Keywords: $CuSbS_2$ nanoparticles; hot-injection; electrical properties

1. Introduction

As the global economic recovery and the development of science and technology, depletion of non-renewable energy and the environment worsening have become significant obstacles hindering the development of the human existence [1]. Thin film photovoltaic have experienced significant research progress in these years, with copper indium gallium selenium(CIGS) solar cell achieving 21.5% [2] and cadmium telluride (CdTe) solar cell achieving 21.7% [3]. However, the toxic elements (Cd in CdTe) or scarcity of materials (In in CIGS and Te in CdTe) are major problems limiting their widespread scale application [4,5].

In recent years, copper antimony sulfide ($CuSbS_2$), a relatively less investigated ternary I−V−VI_2 chalcogenide, has attracted much attention in photovoltaic field due to its promising light absorb ability [6-8]. $CuSbS_2$ not only has a near-optimal direct band gap between 1.1-1.5 eV proved by both theoretical simulation and experimental investigation, but it also has a strong optical absorption coefficients more than 10^{-4} cm^{-1} [9-12]. In addition, ternary chalcostibite $CuSbS_2$ is indicated as an emerging alternative for CIGS and CdTe, because of its abundant elements with low-toxic and economical compared to the CIGS and CdTe [13,14]. Hence, attracted by its promising application, various film-depositing approaches for $CuSbS_2$ have been reported recently,

*Corresponding author: qfhan@shnu.edu.cn

such as spray pyrolysis [15], thermal evaporation [16,17], chemical bath deposition [18], electrodeposition [17,19] and thermal evaporated Sb_2S_3/Cu layers [13]. lkeda et al. has successfully fabricated a $CuSbS_2$ solar cell with an efficiency of 3.13% [20].

Synthesis nanoparticles is attractive and significant because of its perspective to conveniently produce large area solar cells at low cost by the roll to roll method using nanoparticle ink [21]. Therefore, photovoltaic nanoparticles syntheses attract great interest not only for conventional photovoltaic compounds (CIGS, CdTe) [2,3], but also for potential emerging semiconductor compounds (CZTS(Se), CTSe) that can be used in solar cells applications [22-24].

In this paper, we successfully synthesized high quality $CuSbS_2$ nanoparticles by hot-injection method. Thin $CuSbS_2$ films were successfully drop deposited using $CuSbS_2$ nanoparticles dispersed in toluene on Mo-glass substrate. The current-potential (I-V) curves of the $CuSbS_2$ thin film show an increase in photo-current compared to dark current, suggesting that light inspired electrons on the thin film surface make the film conductivity increased [25]. Especially, dark and photo-currents of the $CuSbS_2$ thin film utilize anhydrous ethylenediamine solution removing ligand are larger than that removing ligand using thermal annealing.

2. Experimental

Copper (I) chloride (CuCl, 97%), antimony (III) chloride ($SbCl_3$, 99%), oleylamine (OLA, content 70%) and sulfur (S, 99.99%) were purchased from Alfa Aesar. Toluene and ethanol were purchased from Sinopharm Chemical Reagent Co. Ltd. All chemicals were used without further purification.

All experiments were conducted in a glove box filled with nitrogen. Syntheses of $CuSbS_2$ nanoparticles were carried utilizing hot-injection method, by injecting sulfur-oleylamine solution into hot copper/antimony-oleylamine solution. The S precursor was prepared by dissolving 1 mmol sulfur power into 3 mL oleylamine. Metal precursor was prepared by adding 0.45 mmol Copper (I) chloride, 0.45 mmol antimony (III) chloride and 7 mL OLA, and then vigorously stirred at 100 °C for 2 h. After that, the metal precursor was heat to 240 °C, where 3 ml sulfur precursor was injected. Then the solution turns dark, and the temperature was held at 240 °C for 5 minutes. The mixture was naturally cooled to 60 °C, and 15 ml ethanol was added to the reaction mixture in order to wash off the impurities. The nanoparticles were collected using centrifuge at 8000 rpm for 3 minutes. Supernatant was discarded and the centrifugation process was carried out 2 more times to remove any ligands. The black nanoparticles were dispersed in toluene to form an ink solution.

The $CuSbS_2$ thin films were fabricated by dripping the concentrated nanoparticles dispersions in toluene onto the Mo-coated soda-lime glass substrates, and then drying them at room temperature in vacuum. For removing ligands on nanoparticles surface, two processes were used separately: (1) The films were subjected to a post-annealing process which was conducted at 350 °C for 5 min on a hot plate in N_2 filled glove box. (2) The films were dip in anhydrous ethylenediamine solution for 5 min, and then put it on a hot plate at 100 °C for 5 min.

The crystal structures of the nanoparticles were characterized by D8 Focus X-ray diffraction (XRD) and Raman spectra (RenishawinVia Raman spectrometer) with an incident laser of 514.5 nm. High-resolution transmission electron microscopy (HRTEM) images were acquired on a JEM-2100 microscope and the samples were prepared by drop-casting from toluene dispersions onto Cu grids.

An energy dispersive spectrometer equipped with a field emission scanning electron microscope (Hitachi S-4000) was used to obtain the chemical compositions of the nanoparticles. UV-vis absorbance of the nanoparticles dispersions were detected by Beckman Coulter DU730. The current–voltage curves were recorded using Keithley 2400 Source Meter in dark or under illumination with a xenon lamp at 100mW cm^{-2} (AM1.5). The scan voltage was tuned from -0.5 V to 0.5 V.

3. Results and discussion

The XRD pattern shown in Figure 1 of nanoparticles synthesized at 240 °C for 5 min exhibited a typical diffraction patterns of chalcostibite $CuSbS_2$, which is in agreement with the standard JCPDS card No. 88-0822 of orthorhombic $CuSbS_2$ (Chalcostibite) without any appreciable reflections of other compounds. The lattice constants for the $CuSbS_2$ nanoparticles are determined to be 6.016 Å (a), 3.796 Å (b), and 14.499 Å (c), which are comparable with the values reported for the bulk. In addition to the XRD results, the sample was further studied by Raman spectroscopy (Fig. 2). The Raman spectrum contains an intense peak at approximately 329 cm^{-1}, and two relatively small peaks at approximately 156 cm^{-1} and 251 cm^{-1}, which are in good agreement with a previous report for chalcostibite $CuSbS_2$ [26]. The XRD results and Raman spectrum indicate that pure $CuSbS_2$ was successfully synthesized by hot-injection method.

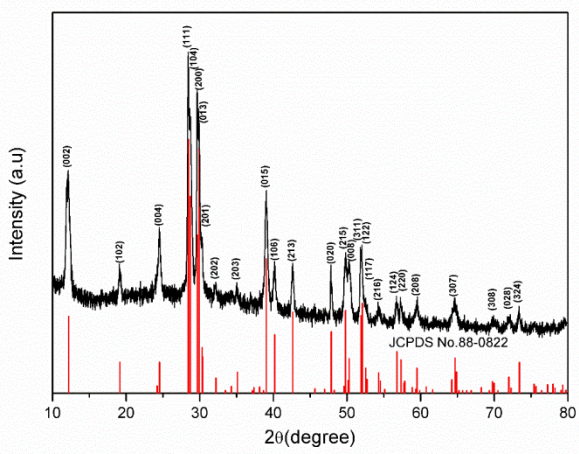

Fig. 1 XRD patterns of the as-deposited $CuSbS_2$ thin film. As a reference, the diffraction pattern of chalcostibite pattern (JCPDS no. 88-0822) is shown

The average elemental composition of as-synthesized $CuSbS_2$ nanoparticles determined by Energy Dispersive X-ray spectroscopy is shown in Figure 3. The S/(Cu+Sb) ratio for $CuSbS_2$ nanoparticles is slightly lower than stoichiometric $CuSbS_2$ because of sulfur loss at higher reaction temperatures.

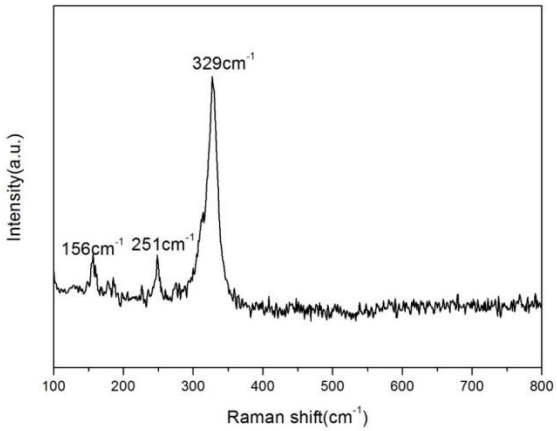

Fig. 2 Ramam spectra of the as-deposited $CuSbS_2$ thin film

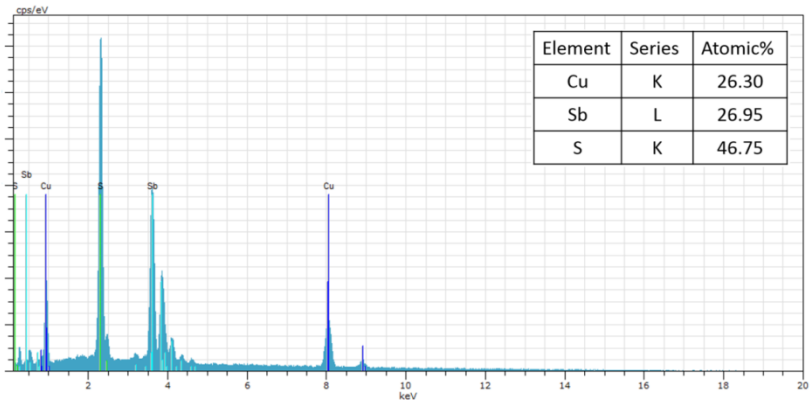

Fig. 3 $CuSbS_2$ nanoparticles determined by Energy Dispersive X-ray spectroscopy

The morphology and size of the nanoparticles are investigated from transmission electron microscope (TEM) images. Figu 4a and b showed TEM images of representative $CuSbS_2$ nanoparticles. Monodispersed spherical particles were observed in the $CuSbS_2$ nanoparticles. Based on corresponding size distribution plots of samples obtained by measuring more than 200 particles, average diameter (d_{av}) of samples was calculated to be around 15 nm. Figure 4c shows the HRTEM image of $CuSbS_2$ nanoparticles, which reveals clear lattice fringes with an average interplanar distance of 0.3 nm, corresponding to (200) planes of orthorhombic $CuSbS_2$. The fast Fourier transform (FFT) image of the HRTEM image shown in Figure 4d exhibits bright spots that correspond to the (111), $(\bar{1}\bar{1}1)$, $(\bar{2}1\bar{3})$, $(2\bar{1}3)$, $(1\bar{2}2)$ and $(\bar{1}2\bar{2})$ reflections of orthorhombic $CuSbS_2$.

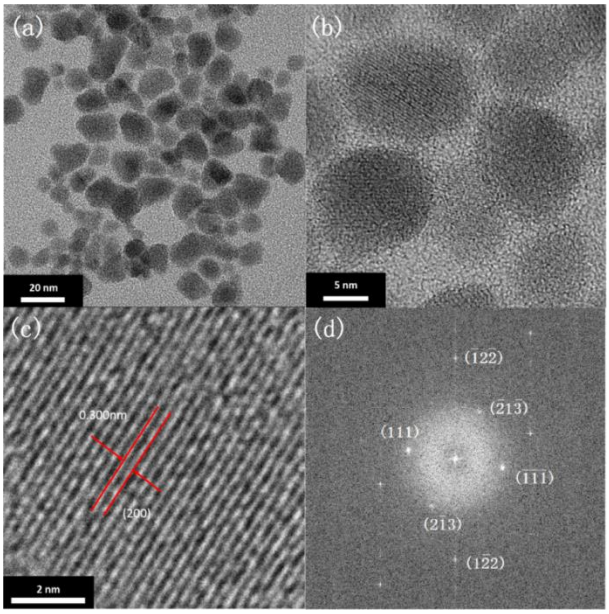

Fig. 4 (a) and (b) TEM images of $CuSbS_2$ nanoparticles with diameters around 15 nm. (c) HRTEM images of $CuSbS_2$. (d)Fast Fourier transformation (FFT) images of HRTEM images shown in panels

The band gap of $CuSbS_2$ nanoparticles is estimated to be 1.26 eV via extrapolating the linear region of the plot of $(ah\nu)^2$ versus photonenergy ($h\nu$) as illustrated in the inset of Figure 5. The band gap value is close to the previous literature for $CuSbS_2$ [27].

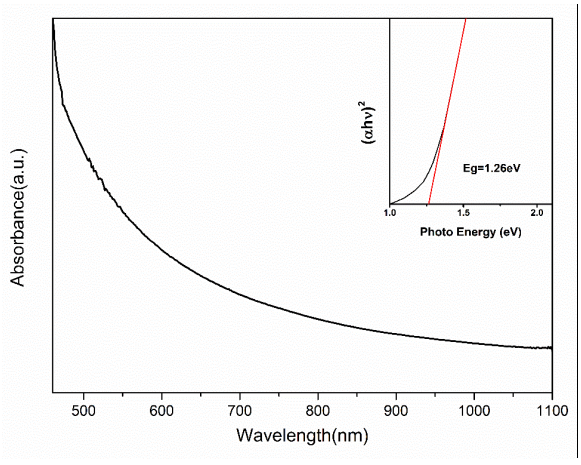

Fig. 5 UV-VIS-NIR spectroscopic characterization of the $CuSbS_2$ nanoparticles

Photoelectrical properties of $CuSbS_2$ films deposited by nanoparticles were further investigated. In order to improve conductivity of the films, we use thermal annealing and anhydrous ethylenediamine solution methods to remove ligand on $CuSbS_2$ surface. As shown in Figure 6, the photocurrents of the films removing ligand by 300 °C thermal annealing and treated with anhydrous

ethylenediamine solution show over 3.9 and 2.1 times increase compared to dark current, respectively. However, the photocurrent of film treated with anhydrous ethylenediamine solution is much larger than the sample annealed at 300 ºC indicates that the conductivity of the film trated with anhydrous ethylenediamine solution is higher than that after thermal annealing. We can observe a XRD diffraction peak attributed to CuS shown in Figure 7, so the relatively high resistance might be caused by the impurity. Different from thermal annealing, anhydrous ethylenediamine solution can effectively remove ligands and keep material structure stable. The light current is larger than that of CZTS, which is about 90 μA current under same test condition [28]. This fact proves that $CuSbS_2$ thin film has good photoelectric properties and large potential in optoelectronic field.

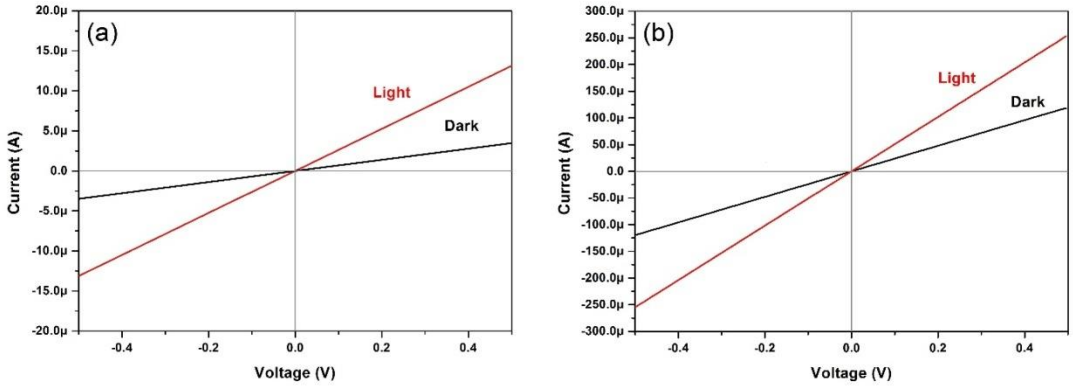

Fig. 6 The current–potential (I–V) curves of the $CuSbS_2$ films remove ligand made from (a) Under the 300°C annealing, (b) dip in anhydrous ethylenediamine solution (tested in the dark (black) and under illumination (red)).

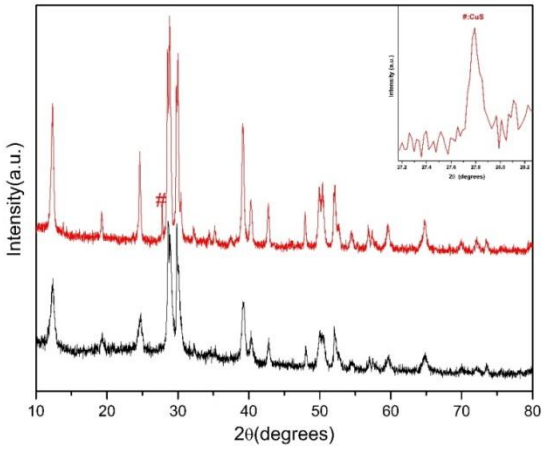

Fig. 7 XRD patterns of the $CuSbS_2$ thin film treated with anhydrous ethylenediamine solution (black) and after thermal annealing (red)

4. Conclusions

In summary, a facile colloidal synthesis of $CuSbS_2$ nanoparticles by simple hot-injection method is described. The XRD pattern of the synthesized $CuSbS_2$ nanoparticles reveals that they correspond well to chalcostibite structure, and the TEM image displays a clear crystalline surface with the interplanar spacing of 0.3 nm, which is good coincidence with the (200) plane of chalcostibite phase $CuSbS_2$. A band gap of 1.26 eV is obtained from the UV-VIS-NIR spectrum. The film prepared by casting the ink containing $CuSbS_2$ nanoparticles demonstrates a notable and stable photo response. Compared with the thermal annealing removing ligand, the dark and light currents of the $CuSbS_2$ thin film utilize anhydrous ethylenediamine solution treated is larger, reveal a high light currents of 253 μA at 0.5 bias. This work shows that $CuSbS_2$ nanoparticles have potential for solar cell absorption material.

Acknowledgements

This work was financially supported by Innovation Program of Shanghai Municipal Education Commission (No. 14YZ079) and Shanghai Municipal Natural Science Foundation (14ZR1430500).

References

[1] M. Z. Jacobson, M. A. Delucchi, Energy Policy **39**, 1154 (2011).
[2] P. Jackson, D. Hariskos, R. Wuerz, O. Kiowski, A. Bauer, T. M. Friedlmeier, M. Powalla, Phys. Status Solidi RRL **9**, 28 (2015).
[3] J. D. Major, R. E. Treharne, L. J. Phillips, K. Durose, Nature. **511**, 334 (2014).
[4] K. Ramanathan, M. A. Contreras, C. L. Perkins, S. Asher, F. S. Hasoon, J. Keane, D. Young, M. Romero, W. Metzger, R. Noufi, J. Ward, A. Duda, Prog. Photovolt: Res. Appl. **11**, 225 (2003).
[5] D. Bonnet, Thin Solid Films **361**, 547 (2000).
[6] D. J. Temple, A. B. Kehoe, J. P. Allen, G. W. Watson, D. O. Scanlon, J. Phys. Chem. C **116**, 7334 (2012).
[7] C. Yan, Z. Su, E. Gu, T. Cao, J. Yang, J. Liu, F. Liu, Y. Lai, J. Li, Y. Liu, RSC Adv. **2**, 10481 (2012).
[8] J. T. R. Dufton, A. Walsh, P. M. Panchmatia, L. M. Peter, D. Colombara, M. S. Islam, Phys. Chem. Chem. Phys. **14**, 7229 (2012).
[9] W. Shockley, H. J. Queisser, J. Appl. Phys. **32**, 510 (1961).
[10] J. Zhou, G. Q. Bian, Q. Y. Zhu, Y. Zhang, C. Y. Li, J. Dai, J. Solid State Chem. **182**, 259 (2009).
[11] Y. R. Lazcano, M. T. S. Nair, P. K. Nair, Mod. Phys. Lett. B **15**, 667 (2001).
[12] Y. R. Lazcano, M. T. S. Nair, P. K. Nair, J. Cryst. Growth. **223**, 399 (2001).
[13] C. Garza, S. Shaji, A. Arato, E. P. Tijerina, G. A. Castillo, T. K. D. Roy, B. Krishnan: Sol. Energy Mater. Sol. Cells, **95**, 2001 (2011).

[14] S. A. Manolache, L. Andronic, A. Duta, A. Enesca, J. Optoelectron. Adv. Mater. **9**, 1269 (2007).
[15] S. A. Manolache, A. Duta, J. Optoelectron. Adv. Mater. **10**, 3219 (2007).
[16] A. Rabhi, M. Kanzari, B. Rezig, Thin Solid Films **517**, 2477(2009).
[17] D. Colombara, L. M. Peter, K. D. Rogers, J. D. Painter, S. Roncallo, Thin Solid Films **519**, 7438 (2011).
[18] S. C. Ezugwu, F. I. Ezema, P. U. Asogwa, Chalcogenide Lett., **7**, 341 (2010).
[19] D. Colombara, L. M. Peter, K. D. Rogers, K. Hutchings, J. Solid State Chem. **186**, 36 (2012).
[20] W. Septina, S. Ikeda, Y. Iga, T. Harada, M. Matsumura, Thin Solid Films, **550**, 700 (2014).
[21] S. E. Habas, H. A. S. Platt, M. F. A. M. Hest, D. S. Ginley, Chem. Rev. **110**, 6571 (2010).
[22] K. Ramasamy, M. A. Malik, P. O'Brien, Chem. Commun. **48**, 5703 (2012).
[23] K. Ramasamy, M. A. Malik, P. O'Brien, Chem. Sci. **2**, 1170 (2011).
[24] W. Wang, M. T. Winkler, O. Gunawan, T. Gokmen, T. K. Todorov, Y. Zhu, D. B. Mitzi, Adv. Energy Mater. **4**, 1301465 (2014).
[25] X. Lu. Z. Zhuang. Q. Peng, Y. Li, Chem. Commun, **47**, 3141 (2011).
[26] Chalcostibite R060262. http://rruff.info/chalcostibite/R060262.
[27] K. Ramasamy, H. Sims, W. H. Butler, A. Gupta, Chem. Mater. **26**, 2891 (2014).
[28] Y. Li, Q. Han, T. W. Kim, W. Shi, Nanoscale. **6**, 3777 (2014).